Improved Post–Detection Processing for Limiter–Discriminator Detection of CPM in a Rayleigh, Fast Fading Channel

David K. Asano, *Member, IEEE* and Subbarayan Pasupathy, *Fellow, IEEE*

Abstract— **A simple, robust processing strategy, called the Fading Magnitude – Integrate, Sample and Dump (FM–ISD) processor, is proposed for use with Limiter–Discriminator detection of CPM signals in Rayleigh, fast fading channels. The FM–ISD processor is introduced as a simplification of an optimal estimator–correlator receiver. The performance is compared to a standard integrator processor and found to provide an improvement in performance for all values of signal–to–noise ratio. The FM–ISD processor is also shown to be robust to changes in modulation format, channel fading rate and pre–detection filter type.**

I. Introduction

Recently, much effort has been put into simple demodulation techniques for mobile communication systems. A notable example is the limiter-discriminator (L-D) combination [1] – [15]. This technique has the advantage of being very robust, which is necessary in fading environments, and very simple, which makes it attractive for portable and handheld devices.

In this paper, we examine the post-detection processing problem in fast, Rayleigh fading environments. In particular, we introduce a simple, robust processing strategy and evaluate its performance with Continuous Phase Modulation (CPM) schemes. We restrict our attention to CPM schemes because of the properties of CPM which make it a good choice for communication over fading channels: bandwidth efficiency and constant envelope.

The performance of the communication systems examined in this paper was found by using computer simulations. Each system was implemented digitally using the Signal Processing Worksystem (SPW^{TM}) [1] from Comdisco Systems. The error probabilities were then found using Monte Carlo simulations. The reason for using simulations is that analytical techniques are difficult to apply and subject to simplifying assumptions. For fast fading environments, the complexity is increased further. Also, if some simplifying assumptions are used, important effects may be lost.

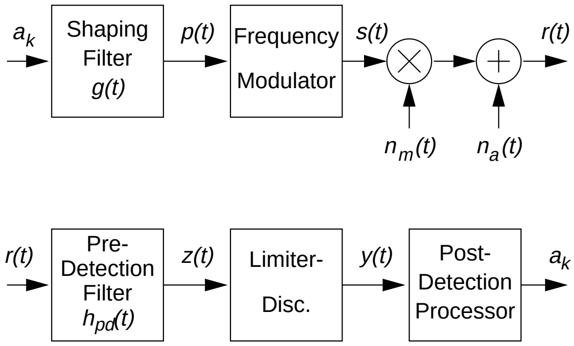

Fig. 1. Communication system model.

The communication system used in this paper is described in section II. In section III, we introduce a new processing strategy and evaluate its performance. In section IV, we examine the robustness of the new processor. Finally, we summarize with some conclusions in section V.

II. System Model and Parameters

The communications system that is used in this paper is shown in Fig. 1. A data source produces equiprobable symbols, $a_k \in \{-1, 1\}$, every symbol interval, T, seconds. These symbols are fed into a shaping filter with impulse response $g(t)$. For a memory length equal to L, $g(t)$ is zero outside the interval $[0, LT]$ and is normalized so that its area is equal to $1/2$.

The output of the shaping filter is given by

$$p(t) = \sum_k a_k g(t - kT). \tag{1}$$

A frequency modulator with deviation constant, h, produces the transmitted signal which is given in complex envelope notation by

$$s(t) = A e^{j\theta(t)}. \tag{2}$$

The amplitude, A, is a constant and $\theta(t)$ is the continuous phase given by

$$\theta(t) = 2\pi h \sum_k a_k \int_{kT}^{t} g(\tau - kT) d\tau. \tag{3}$$

The energy per bit of the modulated signal is denoted by E_b.

Manuscript received August 31, 1993; revised February 10, 1995. This work was supported in part by the Natural Sciences and Engineering Research Council of Canada.

D. Asano is with the Communications Research Laboratory, Ministry of Posts and Telecommunications, 4-2-1, Nukui-Kitamachi, Koganei, Tokyo 184, Japan.

S. Pasupathy is with the Department of Electrical and Computer Engineering, University of Toronto, Toronto, ON M5S 1A4, Canada.

IEEE Log Number 9412996

[1]Signal Processing Worksystem is a Registered Trademark and SPW is a Trademark of Comdisco Systems Inc.

The channel is modelled as consisting of additive and multiplicative noise components, which are both Gaussian distributed and complex. The additive noise component, $n_a(t)$ has a white power spectral density equal to N_0, while the multiplicative component, $n_m(t)$, is generated by passing the same kind of white noise through a filter whose transfer function is given by

$$|H_f(f)|^2 = \begin{cases} \dfrac{H_0}{\sqrt{1-\left(\frac{f}{B_f}\right)^2}} & |f| < B_f \\ 0 & otherwise \end{cases} \tag{4}$$

where H_0 is a constant and B_f is the fading bandwidth. This produces Rayleigh fading with a standard power spectrum for the signal envelope [16], since the multiplicative noise can be written as

$$n_m(t) = \rho(t)\mathrm{e}^{j\psi(t)}, \tag{5}$$

where $\rho(t)$ is Rayleigh distributed and $\psi(t)$ is uniformly distributed in $[-\pi, \pi]$.

Since the amplitude of the received signal varies due to the fading, the signal–to–noise ratio must be averaged over the fading values [17]. This results in

$$\overline{SNR} = \langle |n_m(t)|^2 \rangle E_b/N_0, \tag{6}$$

where $\langle |n_m(t)|^2 \rangle$ is the average value of the squared magnitude of the multiplicative noise.

The signal presented to the receiver can be written as

$$r(t) = s(t)n_m(t) + n_a(t). \tag{7}$$

The receiver begins by removing out–of–band interference with a pre–detection filter. The L–D detector converts the modulated signal to baseband and the post–detection processor produces estimates, $\hat{a}_k$, of the input symbols, a_k.

III. The FM–ISD Processor

In this section, we introduce a new post–detection processor which we refer to as the *Fading Magnitude – Integrate, Sample and Dump (FM–ISD)* processor. Before looking at its performance, we first develop the FM–ISD processor as a simple compromise to an optimal processor for fading environments.

An optimal processor for detection of a random signal in Gaussian noise would generate an estimate of the random signal and then correlate the estimate with the received signal. This is referred to as an estimator–correlator receiver [18]. To implement the estimator–correlator receiver in our case requires the use of estimates of the magnitude and phase of the fading process and knowledge of the effects of the limiter–discriminator combination on the signal. This operation is complicated and the performance is generally very sensitive to the estimate of the fading process. Therefore, this kind of receiver is not suitable for fading environments, where robustness and simplicity are important.

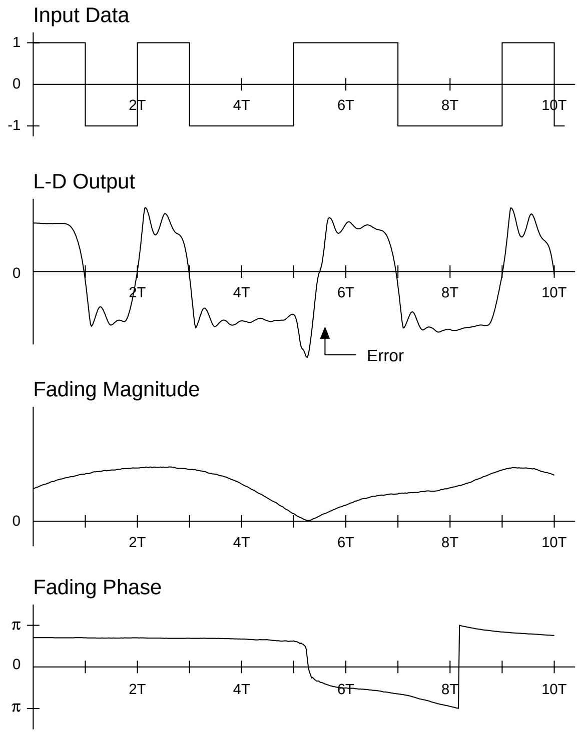

Fig. 2. Distortion of baseband signal due to fading and ISI.

In order to simplify the estimator–correlator receiver, we examine the fading process and the output of the discriminator in more detail when no additive noise is present. In the appendix, it is shown that the output of the pre–detection filter can be written as

$$z_k(t - kT) = A \sum_{i=0}^{k} \eta_i(t - iT)\mathrm{e}^{j\zeta_i(t-iT)} \tag{8}$$

for the kth symbol interval, i.e., $kT \leq t \leq (k+1)T$, where $\eta_i(t)$ and $\zeta_i(t)$ are respectively the filtered magnitude and phase of the received signal in the ith symbol interval.

For the simple case when only the previous symbol causes significant inter–symbol interference (ISI), (8) can be simplified to

$$\begin{aligned} z_k(t - kT) = A[&\eta_{k-1}(t - (k-1)T)\mathrm{e}^{j\zeta_{k-1}(t-(k-1)T)} \\ &+\eta_k(t - kT)\mathrm{e}^{j\zeta_k(t-kT)}] \end{aligned} \tag{9}$$

It is possible due to the fading that $\eta_{k-1}(t-(k-1)T)$ may become larger than $\eta_k(t - kT)$ for a brief period of time. In this case, the information about the present symbol is lost and signal distortion occurs for that period of time. This situation can arise when the magnitude of the fading process decreases suddenly.

In Fig. 2, we see this effect. The input data, the output of the L–D and the magnitude and phase of the multiplicative noise are shown. The sudden drop in the noise magnitude results in a temporary distortion in the output of the L–D. Since the relative magnitude is important, if the noise magnitude is fairly constant, there will be less distortion than if the magnitude is changing rapidly. After processing, this signal distortion will result in an error.

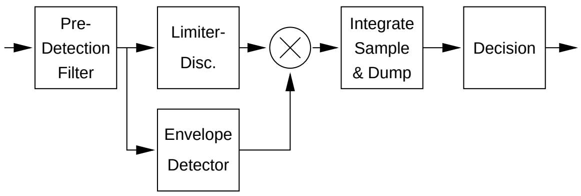

Fig. 3. The FM–ISD processor.

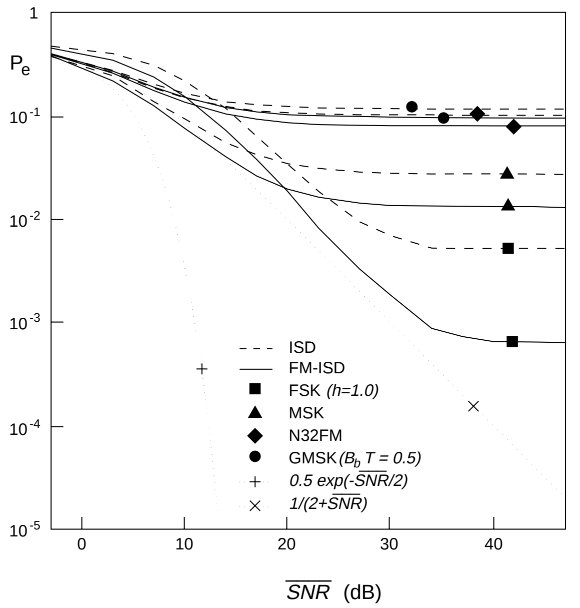

Fig. 4. Performance of the FM–ISD Processor for $B_f T = 0.2$.

This effect can be easily used to modify the estimator–correlator receiver structure. Instead of generating an estimate of the baseband signal, an estimate of the fading magnitude is generated. By correlating the fading magnitude estimate with the received baseband signal, the areas of distortion can be deemphasized, which leads to fewer decision errors and hence to better performance.

An estimate of the fading magnitude is available at the output of the pre–detection filter by simply using an envelope detector. An estimate generated in this way also has the advantage of partially taking into account the ISI caused by the filter. The resulting FM–ISD receiver structure in shown in Fig. 3. The Integrate–Sample–and–Dump (ISD) block consists of an integrator, which integrates the signal over one symbol interval, a sampler, which samples the output of the integrator at the end of the symbol interval, and a dump circuit, which resets the integrator output to zero after the output has been sampled. Note that the FM–ISD processor would be the same as the ISD processor if the output of the envelope detector were a constant.

The performance of the FM–ISD processor is shown in Fig. 4, compared to the performance of an ISD processor, for a fading rate of $0.2/T$. The pre–detection filter that was used is a Gaussian bandpass filter with a $3dB$ bandwidth given by $1/T$. From the figure, we can see that the FM–ISD processor improves the performance of the system for

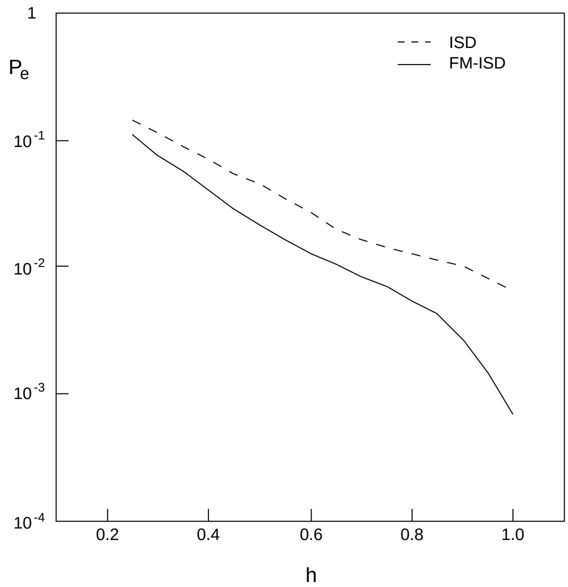

Fig. 5. Performance comparison of the ISD and FM–ISD processors as a function of h for the rectangular pulse shape, $\overline{SNR} = 47dB$ and $B_f T = 0.2$.

all values of $\overline{SNR}$.

Also shown for comparison are the probability of error curves for non–coherent demodulation of Frequency Shift Keying (FSK) with $h = 1.0$, which is non–coherently orthogonal FSK, in additive white Gaussian noise and slow Rayleigh fading channels given by

$$P_e(AWGN) = \frac{1}{2}\exp(-\overline{SNR}/2) \tag{10}$$

and

$$P_e(fading) = 1/(2 + \overline{SNR}) \tag{11}$$

respectively [17].

IV. Robustness of FM–ISD Processor

One of the advantages of the FM–ISD processor is that it is robust in several ways. In this section, we examine the robustness of the FM–ISD processor in terms of modulation format, channel fading rate and pre–detection filter.

A. Modulation Format

The CPM schemes that we considered in this paper are FSK with $h = 1.0$, Minimum Shift Keying (MSK), Gaussian Minimum Shift Keying (GMSK) and Nyquist 32 pulse shaping (N32FM) [19]. The N32FM pulse shape is attractive for integrator–type processors, because N32FM pulses have zero area in adjacent symbol intervals and hence help to reduce ISI.

As shown in Fig. 4, the performance of the communication system with the FM–ISD processor is better than that using the ISD processor for all modulation formats shown. The performance improvement is largest for FSK and smallest for GMSK and N32FM. This can be attributed to the amount of deviation from the center frequency that

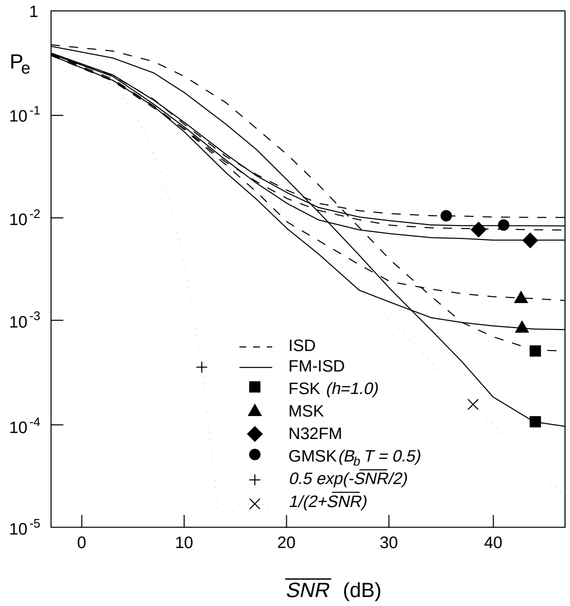

Fig. 6. Performance of the FM–ISD Processor for $B_fT = 0.05$.

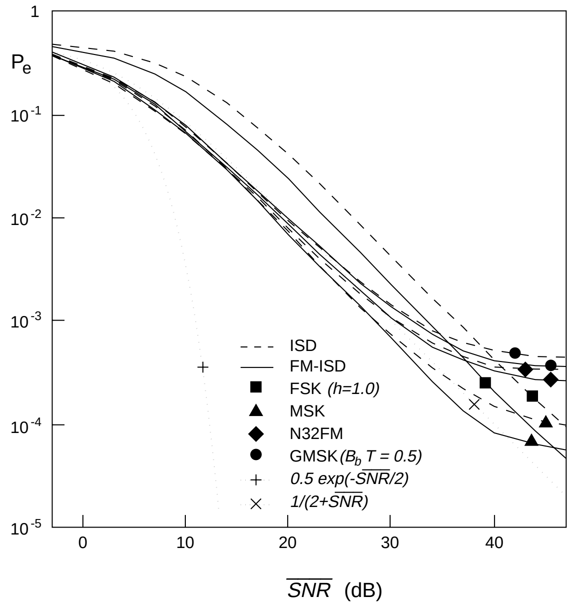

Fig. 7. Performance of the FM–ISD Processor for $B_fT = 0.01$.

each modulation scheme uses. FSK uses a relatively large frequency deviation so the distortion effects can be compensated for. However, GMSK and N32FM use small deviations and hence distortion effects are difficult to correct.

In Fig. 5, the performance of the ISD and FM–ISD processors at high $\overline{SNR}$ is compared as a function of h for the rectangular pulse shape, i.e., the pulse shape used in FSK. From the figure, we can see that the FM–ISD processor provides an improvement for all values of h. The improvement is greatest for larger values of h and gradually decreases as h is lowered.

Since the FM–ISD processor operates to reduce the effects of distortion without using knowledge of the transmitted signal, it does not matter which modulation format is used. This makes the FM–ISD processor robust.

B. Channel Fading Rate

As for the fading rate, we looked at fading rates given by $0.2/T$, $0.1/T$, $0.05/T$, $0.02/T$ and $0.01/T$. These values are representative of fast fading environments.

The results for $0.2/T$, $0.05/T$ and $0.01/T$ are shown in Figs. 4, 6 and 7 for the CPM schemes presented earlier. From these graphs, we can see that the FM–ISD processor provides a performance improvement for all fading rates and modulation schemes. However, as the fading rate is decreased, the performance improvement at low values of $\overline{SNR}$ is reduced. An exception to this is the FSK performance improvement, which is fairly constant for all fading rates shown. This can again be attributed to the relatively large frequency deviation used by FSK.

In the lower $\overline{SNR}$ region, the performance improvement of the FM–ISD processor is reduced because most of the errors are due to the additive noise and not the distortion caused by fading. Thus, as the fading rate is reduced, the effect of the additive noise becomes more dominant over the fading effects.

The performance of all modulation schemes improves as the fading rate is lowered. This was expected since the magnitude of the fading does not vary as much and hence the distortion is reduced. On the other hand, if the distortion is reduced, the ability of the FM–ISD processor to improve performance is also reduced. As the fading rate becomes slower, the performance of the ISD and FM–ISD processors becomes closer and finally, in the limit of no fading, they are the same.

For the range of fading rates examined, the performance at high $\overline{SNR}$ is shown as a function of fading rate in Fig. 8. For GMSK, N32FM and MSK the performance improvement of the FM–ISD processor over the ISD processor is constant. The improvement for FSK is not constant at lower fading rates because the performance at $\overline{SNR} = 47dB$ is not in the error floor region. Although the performance improvement for lower values of $\overline{SNR}$ decreased, the performance improvement in the error floor region is relatively constant.

C. Pre–Detection Filter

Using a different pre–detection filter type, such as a Butterworth filter, has an effect on the performance of the overall system. However, the FM–ISD processor still improves performance relative to the ISD processor as we see in Fig. 9. This is not surprising since the FM–ISD processor does not depend upon the filter type.

As for the bandwidth of the pre–detection filter, the performance improvement obtained by the FM–ISD processor is reduced if the bandwidth is reduced. This effect is seen in Fig. 9. For the larger bandwidth, the FM–ISD processor has better performance than the ISD processor,

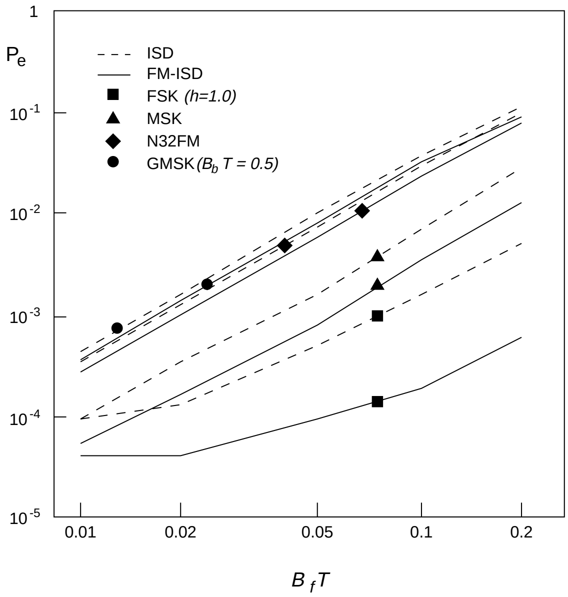

Fig. 8. Performance comparison of the ISD and FM–ISD processors as a function of fading rate for $\overline{SNR} = 47dB$.

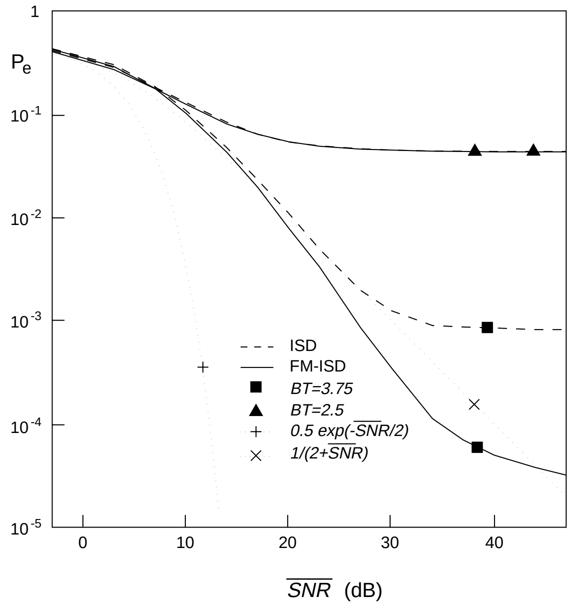

Fig. 9. Performance of the ISD and FM–ISD processors using a 20th order Butterworth pre–detection filter for FSK ($h = 1.0$).

but for the smaller bandwidth, the performance of the two processors is almost the same. This is due to the increase in the amount of ISI generated by the pre–detection filter when the bandwidth is decreased.

V. Conclusions

In this paper, we have introduced a simple, robust post–detection processing strategy, which we refer to as the FM–ISD processor, for use with Limiter–Discriminator detection of frequency modulated signals. The FM–ISD processing strategy is a modification of an optimal estimator–correlator receiver. Instead of using an estimate of the received signal, the FM–ISD processor uses an estimate of the magnitude of the fading, since there is a relationship between the magnitude of the fading and error events. This greatly simplifies the processing circuitry. The FM–ISD processor was shown to improve performance relative to an integrator processor and to be robust to modulation format, channel fading rate and pre–detection filter type.

Appendix
Derivation of Pre–Detection Filter Output

Using (2), (5) and (7), the received signal can be rewritten as

$$r(t) = A\rho(t)e^{j[\theta(t)+\psi(t)]}. \tag{12}$$

The multiplicative noise components $\rho(t)$ and $\psi(t)$, can be written as

$$\rho(t) = \sum_k \rho_k(t-kT) \tag{13}$$

and

$$\psi(t) = \sum_k \psi_k(t-kT), \tag{14}$$

where $\rho_k(t)$ and $\psi_k(t)$ are the magnitude and phase of $n_m(t)$ in the kth symbol interval, i.e.,

$$\rho_k(t-kT) = \begin{cases} \rho(t) & kT \le t \le (k+1)T \\ 0 & \text{otherwise} \end{cases} \tag{15}$$

and

$$\psi_k(t-kT) = \begin{cases} \psi(t) & kT \le t \le (k+1)T \\ 0 & \text{otherwise} \end{cases}. \tag{16}$$

The input to the pre–detection filter, (12), can be rewritten as

$$r(t) = A\sum_k \rho_k(t-kT)e^{j[\theta(t)+\psi_k(t-kT)]}. \tag{17}$$

The output of the pre–detection filter can be expressed as

$$z(t) = \left\{A\sum_k \rho_k(t-kT)e^{j[\theta(t)+\psi_k(t-kT)]}\right\} * h_{pd}(t). \tag{18}$$

Since the filter is linear and time–invariant, the convolution of the sum is equal to the sum of the convolutions so

$$z(t) = A\sum_k \left\{\rho_k(t-kT)e^{j[\theta(t)+\psi_k(t-kT)]}\right\} * h_{pd}(t). \tag{19}$$

Looking at the kth symbol interval, $kT \le t \le (k+1)T$,

$$z_k(t-kT) = A\rho_k(t-kT)e^{j[\theta(t)+\psi_k(t-kT)]} * h_{pd}(t). \tag{20}$$

Representing the filtered magnitude and phase of $z_k(t)$ by $\eta_k(t)$ and $\zeta_k(t)$ respectively,

$$z_k(t) = A\eta_k(t)e^{j\zeta_k(t)}. \tag{21}$$

Note that $\eta_k(t)$ and $\zeta_k(t)$ are non–zero outside $[0,T]$ resulting in inter–symbol interference. Now, (19) can be rewritten as

$$z(t) = A\sum_k \eta_k(t-kT)e^{j\zeta_k(t-kT)}, \tag{22}$$

which for the kth symbol interval results in

$$z_k(t-kT) = A\sum_{i=0}^{k}\eta_i(t-iT)e^{j\zeta_i(t-iT)} \tag{23}$$

due to the effects of ISI.

Acknowledgement

The authors would like to thank the reviewers for their comments and suggestions, which have helped us to improve the quality of this paper.

References

[1] S. M. Elnoubi, "Probability of error analysis of digital partial response continuous phase modulation with noncoherent detection in mobile radio channels," *IEEE Trans. Veh. Technol.*, vol. 38, pp. 19–30, Feb. 1989.

[2] T. T. Tjhung, K. M. Lye, and T. H. Hu, "On discriminator detection of narrowband digital FM in fading channels," *IEICE Trans. E*, vol. E73, pp. 1587–1597, Oct. 1990.

[3] R. F. Pawula, "On the theory of error rates for narrowband digital FM," *IEEE Trans. Commun.*, vol. COM-29, pp. 1634–1643, Nov. 1981.

[4] S. M. Elnoubi and S. Gupta, "Error rate performance of noncoherent detection of duobinary coded MSK and TFM in mobile radio communication systems," *IEEE Trans. Veh. Technol.*, vol. 30, pp. 62–70, May 1981.

[5] N. A. B. Svensson and C.-E. Sundberg, "Performance evaluation of differential and discriminator detection of continuous phase modulation," *IEEE Trans. Veh. Technol.*, vol. 35, pp. 106–116, Aug. 1986.

[6] I. Korn, "M-ary frequency shift keying with limiter discriminator integrator detector in satellite mobile channel with narrowband receiver filter," *IEEE Trans. Commun.*, vol. COM-38, pp. 1771–1778, Oct. 1990.

[7] P. Varshney and S. Kumar, "Performance of GMSK in a land mobile radio channel," *IEEE Trans. Veh. Technol.*, vol. 40, pp. 607–614, July 1991.

[8] I. Korn, "GMSK with limiter discriminator detection in satellite mobile channel," *IEEE Trans. Commun.*, vol. COM-39, pp. 94–101, Jan. 1991.

[9] S. M. Elnoubi, "Analysis of GMSK with discriminator detection in mobile radio channels," *IEEE Trans. Veh. Technol.*, vol. 35, pp. 71–76, May 1986.

[10] S. M. Elnoubi, "Predetection filtering effect on the probability of error of GMSK with discriminator detection in mobile radio channels," *IEEE Trans. Veh. Technol.*, vol. 37, pp. 104–107, May 1988.

[11] T. T. Tjhung, K. M. Lye, K. A. Koh, and K. B. Chang, "Error rates for narrow-band digital FM with discriminator detection in mobile radio systems," *IEEE Trans. Commun.*, vol. COM-38, pp. 999–1005, July 1990.

[12] I. Korn, "GMSK with frequency selective Rayleigh fading and cochannel interference," *IEEE J. Select. Areas Commun.*, vol. SAC-10, pp. 506–515, Apr. 1992.

[13] O. Andrisano, M. Chiani, and R. Verdone, "Performance of narrowband CPM systems with limiter–discriminator–integrator detection and decision feedback equalization in mobile radio channels," *IEEE Trans. Veh. Technol.*, vol. 42, pp. 166–176, May 1993.

[14] J. P. Fonseka, "Baseband pulse shaping to improve M–ary FSK in satellite mobile systems," *IEEE Trans. Veh. Technol.*, vol. 41, pp. 424–429, Nov. 1992.

[15] K. Ohno and F. Adachi, "Performance evaluation of various decision schemes for frequency demodulation of narrow-band digital FM signals in land mobile radio," *IEEE Trans. Veh. Technol.*, vol. 39, pp. 109–116, May 1990.

[16] J. D. Parsons, *Mobile communication systems.* New York: Wiley, 1989.

[17] J. Proakis, *Digital Communications.* New York: McGraw-Hill, 1983.

[18] H. L. Van Trees, *Detection, Estimation and Modulation Theory: Part III.* New York: John Wiley & Sons, 1971.

[19] B. Sayar and S. Pasupathy, "Nyquist 3 pulse shaping in Continuous Phase Modulation," *IEEE Trans. Commun.*, vol. COM-35, pp. 57–67, Jan. 1987.

David K. Asano (SM'88–M'95) received the B.A.Sc. degree (with honours) from the University of British Columbia, Vancouver, Canada in 1985, and the M.A.Sc. and Ph.D. degrees from the University of Toronto, Toronto, Canada, all in Electrical Engineering. He was involved in Northern Telecom's Network Engineering Program as an Assistant Coordinator in 1990 and 1991 and as a lecturer from 1990 to 1993. From 1990 to 1992 he managed the Communications Group computer system at the University of Toronto. He was a teaching assistant at the University of Toronto from 1988 to 1994.

Currently, he is an STA Fellow at the Communications Research Laboratory of the Ministry of Posts and Telecommunications in Koganei, Japan. He is working on coding and modulation techniques for fading channels as well as intelligent communication systems.

Subbarayan Pasupathy (M'73–SM'81–F'91) was born in Madras, Tamilnadu, India on September 21, 1940. He received the B.E. degree in telecommunications from the University of Madras in 1963, the M.Tech. degree in electrical engineering from the Indian Institute of Technology, Madras, in 1966, and the M.Phil. and Ph.D. degrees in engineering and applied science from Yale University in 1970 and 1972, respectively.

He joined the faculty of the University of Toronto in 1973 and became a Professor of Electrical Engineering in 1983. He has served as the Chairman of the Communications Group and as the Associate Chairman of the Department of Electrical Engineering at the University of Toronto. His research interests are in the areas of communication theory, digital communications and statistical signal processing. He is a registered Professional Engineer in the province of Ontario. During 1982–1989 he was an Editor for *Data Communications and Modulation* for the IEEE Transactions on Communications. He has also served as a Technical Associate Editor for the IEEE Communications Magazine (1979–1982) and as an Associate Editor for the Canadian Electrical Engineering Journal (1980–1983). Since 1984, he has been writing a regular column entitled "Light Traffic" for the IEEE Communications Magazine.

Dr. Pasupathy was elected as a Fellow of the IEEE in 1991 for "contributions to bandwidth efficient coding and modulation schemes in digital communication."